Effect of topology upon relay synchronization in triplex neuronal networks

Cite as: Chaos **30**, 051104 (2020); https://doi.org/10.1063/5.0008341
Submitted: 20 March 2020 . Accepted: 20 April 2020 . Published Online: 07 May 2020

Fenja Drauschke, Jakub Sawicki, Rico Berner, Iryna Omelchenko, and Eckehard Schöll

Effect of topology upon relay synchronization in triplex neuronal networks

Cite as: Chaos **30**, 051104 (2020); doi: 10.1063/5.0008341
Submitted: 20 March 2020 · Accepted: 20 April 2020 ·
Published Online: 7 May 2020 · Publisher error corrected: 12 May 2020

Fenja Drauschke,[1] Jakub Sawicki,[1] Rico Berner,[1,2,a)] Iryna Omelchenko,[1] and Eckehard Schöll[1,b)]

AFFILIATIONS

[1]Institut für Theoretische Physik, Technische Universität Berlin, Hardenbergstr. 36, 10623 Berlin, Germany
[2]Institut für Mathematik, Technische Universität Berlin, Strasse des 17. Juni 136, 10623 Berlin, Germany

[a)]**Electronic mail:** rico.berner@physik.tu-berlin.de
[b)]**Author to whom correspondence should be addressed:** schoell@physik.tu-berlin.de

ABSTRACT

Relay synchronization in complex networks is characterized by the synchronization of remote parts of the network due to their interaction via a relay. In multilayer networks, distant layers that are not connected directly can synchronize due to signal propagation via relay layers. In this work, we investigate relay synchronization of partial synchronization patterns like chimera states in three-layer networks of interacting FitzHugh–Nagumo oscillators. We demonstrate that the phenomenon of relay synchronization is robust to topological random inhomogeneities of small-world type in the layer networks. We show that including randomness in the connectivity structure either of the remote network layers or of the relay layer increases the range of interlayer coupling strength where relay synchronization can be observed.

The investigation of synchronization in networks of coupled oscillatory units is a vivid research area with broad applications in nature and technology.[1,2] Uncovering complex mechanisms leading to coexistent synchrony and asynchrony plays an important role in our understanding of many biological[3] and technological systems.[4,5] Collective phenomena such as remote synchronization where distant parts of complex networks synchronize despite the absence of a direct connection is a challenging problem. In particular, in multilayer networks, remote layers can synchronize due to their interaction through intermediate (relay) layers. Such scenarios have been observed in the setting of multiplex networks.[6] These are special multilayer networks, where each layer contains the identical set of nodes and only one-to-one connections between the corresponding nodes in the neighboring layers are allowed. Depending on the type of network nodes and intralayer topologies, complex partial synchronization patterns such as clusters, chimera states, or solitary states can be formed inside the layers. Only recently, relay synchronization of chimera states, i.e., states with spatially coexisting coherent and incoherent domains, has been explored and shown to be of interest for a wide range of applications.[7] In the present work, we analyze the robustness of the relay synchronization of chimera states in three-layer multiplex networks of FitzHugh–Nagumo (FHN) oscillators, which are a paradigmatic model widely used in neuroscience. We find that relay synchronization is sensitive to changes in the connectivity of the remote layers as well as the relay layer.

I. INTRODUCTION

The analysis of complex networks is of great interest with respect to various real-world systems such as social networks,[8] economics,[9] ecology,[10] finance,[11] transport systems,[12,13] and the neural activity in the brain.[14–17] Many of such systems can be represented as multilayer networks,[18,19] where elements are organized in layers with different types of interaction within and between the layers. Multiplex networks represent a special type of multilayer structures, where each layer contains the same number of nodes and only one-to-one connections between equivalent nodes from neighboring layers are permitted. Multiplex networks can be associated with social and technological systems,[20] for instance, with dynamical processes where layers correspond to the states of the system at different times,[21] or with different types of links. Multilayer structures allow for full[22] or partial[23] synchronization between the layers, and different synchronization scenarios can be observed, such as explosive synchronization.[24]

An intriguing phenomenon in networks with multiplex topology is relay (or remote) synchronization between layers that are not directly connected and interact via an intermediate (relay) layer. This can occur in single systems, such as lasers[4] and electronic circuits,[5] as well as in networks between remote pairs of nodes.[25–27] Moreover, the phenomenon of relay synchronization might be associated with an enhancement of synchronization in complex networks with heterogeneous units.[27] Recently, relay synchronization has also been demonstrated in remote pairs of layers,[6,7,28–30] where in Ref. 6 complex topologies like Erdös–Renyi and scale-free were studied. Relay synchronization allows for distant coordination, which may be applied to encryption key distribution and secure communication.[28] Beside this, it is of great relevance in human brain networks, where the thalamus[31] and the hippocampus[3] are known to act as a relay between different brain areas. The human brain is organized by small-world topologies on the macro- and on the micro-scale.[32,33] Therefore, in this paper, we generalize our previous work on relay synchronization, which used simple nonlocally coupled ring networks,[7] to more complex, small-world-like topologies. Thereby, we also gain a deeper understanding of the underlying mechanisms of relay synchronization, which could give insight into the functionality of certain brain processes.

With regard to relay synchronization in complex networks, Ref. 27 has revealed the significance of network structural and dynamical symmetries for the appearance of distant synchronization. However, while some dynamical aspects of remote synchronization of individual nodes have been uncovered,[6,25,34] very little is known about relay synchronization of partial synchronization patterns. Prominent examples of such patterns are chimera states, characterized by the coexistence of synchronized (coherent) and desynchronized (incoherent) spatial domains. Chimera states were found in a plethora of networks of coupled oscillators.[35–41] The coexistence of synchrony and asynchrony in the brain is reminiscent of the phenomenon of unihemispheric sleep.[17,42–44] Similarly, during perceptual organization,[45] behavioral sensation,[46,47] and epileptic seizures,[16,48,49] partially synchronized patterns arise, which can be associated with chimera states. Chimera patterns have been numerically observed in networks of coupled neurons with nonlocal topologies.[50–54]

The purpose of this work is to uncover the effects of the layer topologies upon the scenarios of relay synchronization in a three-layer network consisting of FitzHugh–Nagumo oscillators.[55] Here, the individual layers are initially organized as nonlocally coupled rings, allowing for the formation of chimera states within the layers.[51,53] In such networks, two remote layers synchronize due to their interaction via the relay layer. Moreover, a special regime of "double chimera" is observed, where only coherent domains of the chimera states synchronize remotely.[7] We examine the robustness of relay synchronization by perturbing the network topologies within the layers. Applying the Watts–Strogatz algorithm,[57] first, we randomly remove links in the remote layers and replace them with random shortcuts. Second, we consider topological inhomogeneity in the relay layer keeping the remote layers as regular rings. Surprisingly, we observe that introducing topological inhomogeneities increases the range of the interlayer coupling strength for which relay synchronization in the network takes place.

II. THE MODEL

We consider a multiplex network consisting of three layers, schematically shown in Fig. 1. Each layer, labeled by $i = 1, 2, 3$, contains N nodes which form a nonlocally coupled ring, where each node is connected with its R nearest neighbors to both sides. Throughout the paper, we fix $N = 500$ and $R = 170$. Between the layers, the nodes are bidirectionally connected with their corresponding counterpart from the neighboring layers. The dynamical variable $\mathbf{x}_k^i = (u_k^i, v_k^i)^T$ of each node is governed by

$$\dot{\mathbf{x}}_k^i(t) = \mathbf{F}(\mathbf{x}_k^i(t)) + \frac{\sigma_i}{R}\sum_{l=1}^{N} a_l^i \mathbf{H}[\mathbf{x}_k^i(t) - \mathbf{x}_k^i(t)] + \sum_{j=1}^{3}\sigma_{ij}\mathbf{H}[\mathbf{x}_k^j(t) - \mathbf{x}_k^i(t)], \quad (1)$$

where $k = 1, \ldots, N$ numbers the nodes, $i = 1, 2, 3$ labels the layer, and $a_{kl}^i \in \{0, 1\}$ are the elements of the adjacency matrix $\mathbf{A}^i$, determining the fundamental topology of layer i, σ_i is the intralayer coupling strength, and σ_{ij} is the interlayer coupling strength. The local dynamics of each oscillator is governed by the FitzHugh–Nagumo (FHN) system,

$$\mathbf{F}(\mathbf{x}) = \begin{pmatrix} \frac{1}{\varepsilon}(u - \frac{u^3}{3} - v) \\ u + a, \end{pmatrix}, \quad (2)$$

where u is the activator (membrane potential) and v is the inhibitor (recovery variable comprising all inhibitory processes). We fix the threshold parameter $a = 0.5$ and the timescale separation parameter $\varepsilon = 0.01$ throughout the paper, ensuring oscillatory dynamics of the individual units. The interlayer coupling scheme for the triplex network is defined as follows:

$$\boldsymbol{\sigma} = \begin{pmatrix} 0 & \sigma_{12} & 0 \\ \sigma_{21} & 0 & \sigma_{23} \\ 0 & \sigma_{32} & 0 \end{pmatrix}. \quad (3)$$

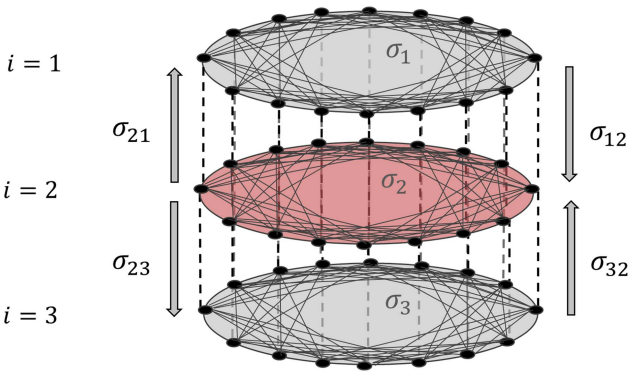

FIG. 1. Illustration of a triplex network with nonlocally coupled ring topology with intralayer coupling strength σ_i and interlayer coupling strength σ_{ij} $(i, j = 1, 2, 3)$. The remote layers $(i = 1, 3)$, depicted in gray, are connected through the relay layer $(i = 2)$, marked in red.

By choosing $\sigma_{12} = \sigma_{32}$ and $\sigma_{21} = \sigma_{23} = \frac{\sigma_{12}}{2}$, the interlayer coupling is bidirectional and has a constant row sum. Throughout this paper, the interaction between the neurons is realized through a rotational coupling matrix in order to include cross coupling between the activator and the inhibitor,

$$\mathbf{H} = \begin{pmatrix} \varepsilon^{-1}\cos\phi & \varepsilon^{-1}\sin\phi \\ -\sin\phi & \cos\phi \end{pmatrix}. \tag{4}$$

Fixing the coupling phase to $\phi = \frac{\pi}{2} - 0.1$ allows for the observation of chimera states within the layers.[51]

To analyze and distinguish different forms of synchronization between the layers in our networks, we employ the following measures. The global interlayer synchronization error E^{ij} quantifies the synchronization between layers i and j,

$$E^{ij} = \lim_{T\to\infty} \frac{1}{NT} \int_0^T \sum_{k=1}^{N} \left\| \mathbf{x}_k^i(t) - \mathbf{x}_k^j(t) \right\| \mathrm{d}t, \tag{5}$$

where $\|\cdot\|$ is the Euclidean norm and $i, j = 1, 2, 3$ denote the layer number.[7] The global interlayer synchronization error is equal to zero when all corresponding oscillators in two layers are synchronized and perform identical dynamics. Based on this measure, one can distinguish the following types of synchronization:

1. *Full interlayer synchronization:* All layers are completely synchronized ($E^{12} = E^{13} = 0$).
2. *Relay interlayer synchronization:* Remote layers are completely synchronized and not synchronized to the relay layer ($E^{13} = 0$ and $E^{12} \neq 0$).
3. *Interlayer desynchronization:* Different patterns in each layer ($E^{12} \neq E^{13} \neq 0$).

While the global interlayer synchronization error gives us information about the complete synchrony of the layers, it is not able to distinguish possible regimes of partial synchronization between the layers. To obtain more detailed information, we analyze the local interlayer synchronization error E_k^{ij} for corresponding pairs of nodes k from two layers,

$$E_k^{ij} = \lim_{T\to\infty} \frac{1}{T} \int_0^T \left\| \mathbf{x}_k^i(t) - \mathbf{x}_k^j(t) \right\| \mathrm{d}t. \tag{6}$$

This measure uncovers complex regimes where only some of the oscillator pairs are synchronized, thus vanishing there.

Nonlocally coupled ring topologies within the layers allow for the observation of chimera states within the layers.[51] An important feature of these patterns is the difference of mean phase velocities for synchronized and desynchronized groups of oscillators.[35,36] Usually, oscillators in synchronized domains are phase-locked and have identical frequencies, while oscillators from the incoherent domain speed up (or slow down) and the mean frequency profile assumes an arc-like shape. The mean phase velocity for each oscillator is calculated as

$$\omega_k = \frac{2\pi M_k}{\Delta T} \quad k = 1, 2, \ldots N, \tag{7}$$

where M_k is the number of complete oscillations of the kth node during the average time ΔT.

III. RESULTS

Before starting to introduce topological inhomogeneities in our network, we address the case of the unperturbed network, where full and partial relay synchronization is observed.[7] In contrast to Ref. 7, the interlayer coupling delay is neglected. The main point of relay synchronization is that the two remote layers are not directly connected but via the relay, which breaks the symmetry of the interlayer couplings between all three layers and assigns a special topological role to the relay as a mediator. As a result, diverse dynamical patterns may arise, including relay synchronization between the outer layers as well as full synchronization between all three layers, or desynchronization, depending upon the interlayer coupling strength. Figure 2 displays averaged results of five numerical simulations

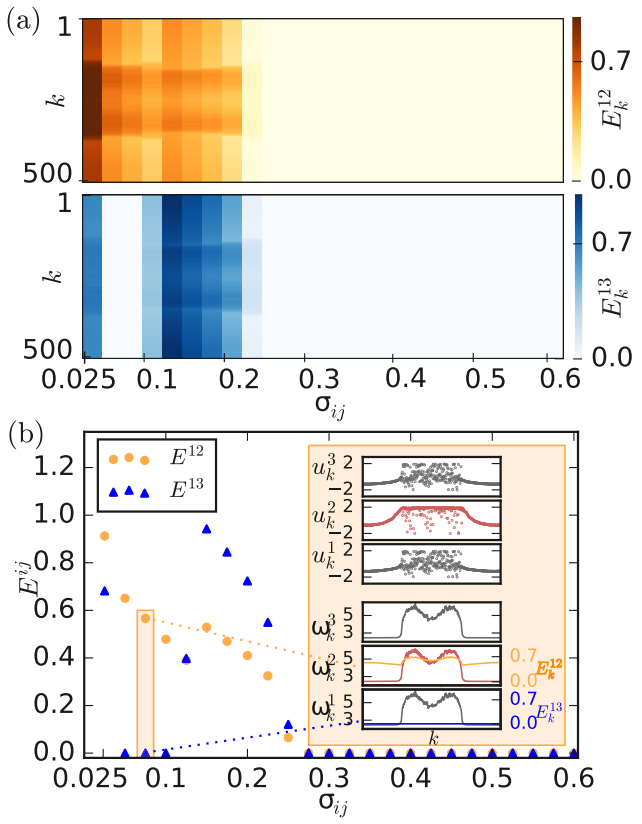

FIG. 2. (a) Local and (b) global synchronization error with identical layers vs interlayer coupling strength $\sigma_{ij} \equiv \sigma_{12} = \sigma_{32}$. For each parameter value we average over 5 sets of random initial conditions, where different realizations are used for the three layers. One can distinguish three regions of dynamics with increasing $\sigma_{ij} \geq 0.05$: (i) relay synchronization, (ii) desynchronization, and (iii) full synchronization. The insets in (b) show snapshots u_k^i and mean phase velocity profiles ω_k^i together with local synchronization errors E_k^{12} (orange) and E_k^{13} (blue) for a coupling strength of $\sigma_{ij} = 0.075$. The relay layer is marked in red and the remote layers in gray. Parameters are $\varepsilon = 0.05$, $a = 0.5$ $R = 170$, $\phi = \frac{\pi}{2} - 0.1$, $N = 500$, $\sigma_i = 0.2$ for layers $i = 1, 2, 3$. The simulation time is $t_{max} = 2000$ with time steps of $\Delta t = 0.05$.

for different sets of random initial conditions for the three-layer network [Eq. (1)]. Figure 2(a) shows the local synchronization errors between the remote layers and the relay layer (upper panel, orange) and between the two remote layers (middle panel, blue) with increasing interlayer coupling strength. Figure 2(b) condenses those results by depicting the global synchronization errors. One can identify three characteristic regimes.[56] In the first one, for small interlayer coupling strength $\sigma_{ij} \equiv \sigma_{12} = \sigma_{32} \geq 0.05$, we observe relay synchronization with zero error E^{13} between the remote layers 1 and 3 and nonzero error E^{12} between the remote and relay layers. In the second regime, with further increase of σ_{ij}, all three layers are desynchronized. Finally, for the large interlayer coupling strength, in the third regime, the whole network is completely synchronized ($E^{12} = E^{13} = 0$). The inset demonstrates an example of relay synchronization for $\sigma_{ij} = 0.075$ [region shaded in orange in panel (b)]: upper panels depict snapshots of chimera states in three layers, and bottom panels show the corresponding mean phase velocity profiles ω_k^i together with local synchronization errors E_k^{ij}.

In the following, we change the connectivities inside the network layers step by step toward a random topology following the Watts–Strogatz algorithm.[57] For this, we introduce the parameter p, which determines the probability for each link of the regular ring to be replaced by a random link and, therefore, serves as a measure for the degree of randomness in the network. First, we investigate the influence of the parameter p on the network properties.

With increasing probability of random shortcuts, we analyze the clustering coefficients C and average shortest path length L within the inhomogeneous layer. Figure 3(a) demonstrates that increasing the randomness p results in a decreasing clustering coefficient, corresponding to the formation of low- and high-degree nodes [Fig. 3(c)] and thus to a growing topological inhomogeneity within one layer. Because of the small ensemble size used for averaging, artifacts may arise, e.g., the data point at $p = 1$ does not continue to decrease. At the same time, we observe an almost constant shortest path length in Fig. 3(a). Due to the large nonlocal coupling range R, the shortest path length is already quite small for the regular ring ($p = 0$) and is not changed much by the introduction of shortcuts. This is in contrast to classical small-world networks that start rewiring from a sparse nonlocally coupled ring network (small coupling range) and hence exhibit a pronounced transition from large C and L (sparse ring) to small C and L (random network) via an intermediate small-world regime with large C and small L. The adjacency matrices of a layer are shown in Fig. 3(b) for different p. For $p = 0$, the matrix is symmetric and contains spatially separated homogeneous regions of coupling (colored) and no coupling (white), representing the regular nonlocally coupled ring. Increasing p leads to the creation of shortcuts in the network, which connect distant spatial domains. In order to examine the influence of p upon the relay synchronization scenario, we focus on the global synchronization error vs the interlayer coupling strength (Fig. 4).[56] In the following, the topology of the layers is modified with the rewiring

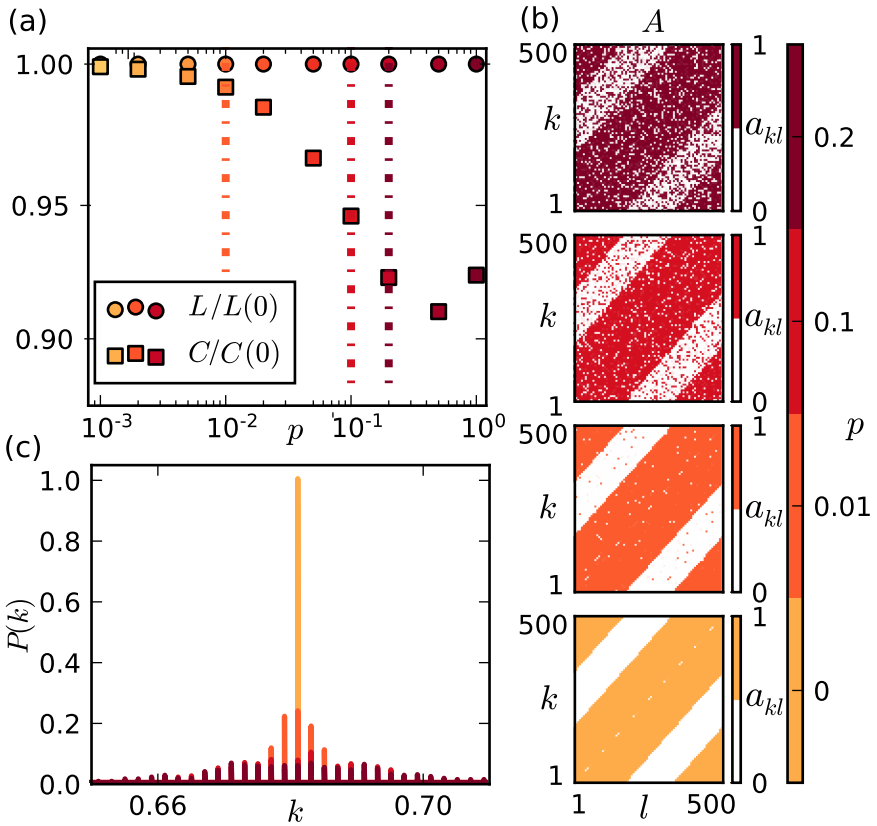

FIG. 3. (a) Normalized shortest path length $L(p)/L(0)$ (circles) and normalized clustering coefficient $C(p)/C(0)$ (squares) averaged over 5 random realizations of the Watts–Strogatz connectivity for increasing rewiring probability p (color coded, see the color scale on the right), generated with the Watts–Strogatz algorithm.[57] (b) $N \times N$-adjacency matrices a_{kl} for different p ($p = 0$, 0.01, 0.1, and 0.2, see color scale on the right). (c) Histograms showing the normalized degree distribution $P(k)$ of a Watts–Strogatz graph with $N = 500$, $R = 170$ and increasing p ($p = 0$, 0.01, 0.1, and 0.2, see the color scale on the right). Other parameters as in Fig. 2.

probability p in two different ways: we either change the topology of the remote layers (applying the same random realization to both layers) or the relay layer while keeping the regular nonlocally coupled ring structure in the relay layer or remote layers, respectively.

Our simulations with random initial conditions show that besides the familiar scenario (relay interlayer synchronization—desynchronization—full interlayer synchronization) observed for the unperturbed three-layer network, frequently a different scenario occurs, where the system changes its dynamics directly from relay to full synchronization without being desynchronized in between. This new transition is shown in Fig. 4. For both cases of inhomogeneity, increasing p leads to a growing global synchronization error E^{12} such that the threshold value of interlayer coupling σ_{ij}^*, up to which the system remains relay-synchronized, before becoming fully synchronized, shifts substantially toward higher values. Snapshots and mean phase velocity profiles with local synchronization errors are shown in the inset, depicting the relay synchronization of chimera states

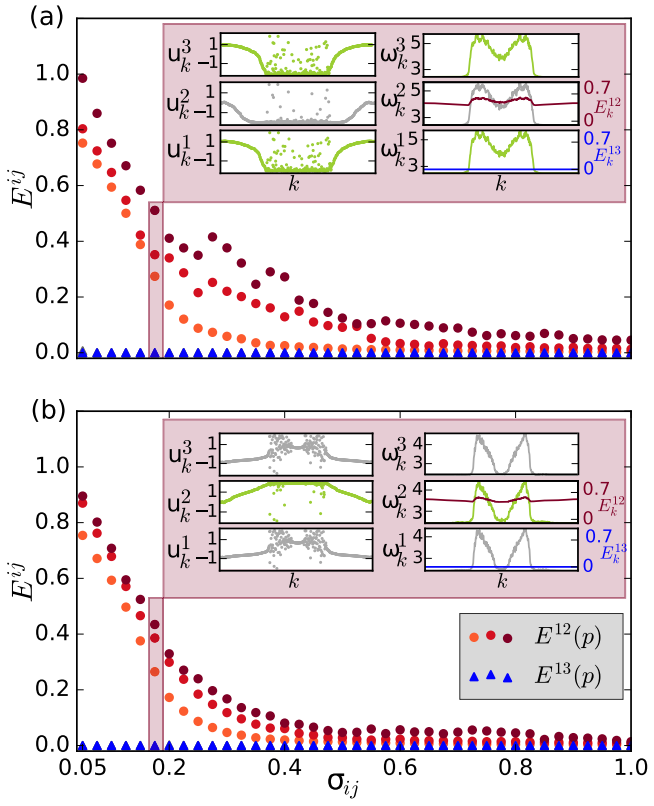

FIG. 4. Global synchronization error E^{ij} vs coupling strength $\sigma_{ij} \equiv \sigma_{12} = \sigma_{32}$, where $E^{13} = 0$ is shown by blue triangles and E^{12} is marked by colored circles for three different values of p ($p = 0.01$, 0.1, and 0.2, color coded as in Fig. 3). For each value of p, we average over five network realizations with different random sets of initial conditions. (a) Topology of the remote layers is modified and (b) topology of the relay layer is changed. The insets show snapshots u_k^j and mean phase velocity profiles ω_k^j with local synchronization errors E_k^{12} (red), E_k^{13} (blue) for all layers for $\sigma_{ij} = 0.175$ and $p = 0.2$. The manipulated layers are marked green. Other parameters as in Fig. 2.

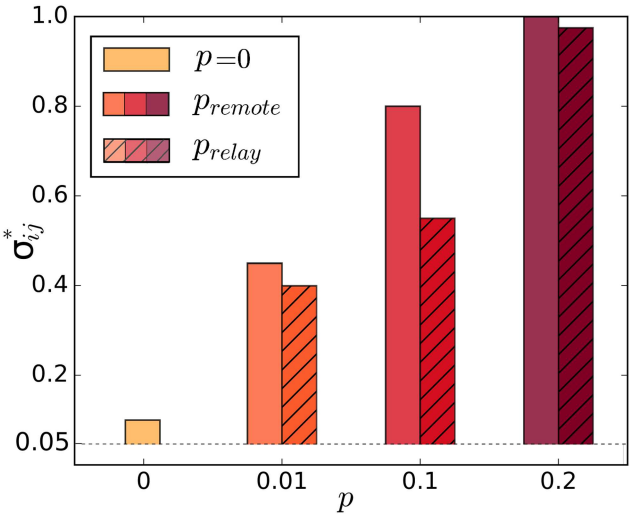

FIG. 5. Threshold value σ_{ij}^* up to which the system remains relay-synchronized depending on the interlayer coupling strength σ_{ij} and the link rewiring probability $p = 0$, 0.01, 0.1, and 0.2. The values $\sigma_{ij}^*(p)$ are calculated from the data of Fig. 4, where the system is assumed to be fully synchronized if $E^{12} \leq 0.02$. The left and right bars refer to inhomogeneous remote (plain) or relay layer (hatched), respectively.

for an interlayer coupling of $\sigma_{ij} = 0.175$ and $p = 0.2$. Here, we further observe the emergence of a two-headed chimera state, i.e., two incoherent domains, in the case of an inhomogeneous relay layer. In the case of inhomogeneous remote layers, the two-headed chimera state is not observed. As it is known from Ref. 51, two-headed chimera states emerge due to a subtle interplay between coupling strength and nonlocality in the coupling structure. Remarkably, the relay layer is more sensitive to the introduction of nonlocality in the sense of Watts and Strogatz. Note that with increasing randomness $p > 0.2$, we find successively shrinking intervals of σ_{ij} for which chimeras exist. Relay synchronization, however, can still be observed. Figure 5 illustrates the results of our numerical simulations for three nonzero values of the link rewiring probability p. It compares the critical interlayer coupling strength σ_{ij}^* at the transition from relay synchronization to complete synchronization, and for comparison also gives the threshold of relay synchronization for $p = 0$. We find that networks with inhomogeneous remote layers have higher thresholds, while the transition to complete synchronization for a network with an inhomogeneous relay layer takes place for slightly lower coupling strengths. Our analysis shows that introducing randomness in the topology of either the remote or the relay layer has an advantageous effect upon the robustness of the regime of relay synchronization in the three-layer network. With increasing rewiring probability, the threshold values of the interlayer coupling strength, up to which the relay-synchronized state is preserved, increase significantly.

IV. CONCLUSION

In summary, we have analyzed nontrivial synchronization scenarios in three-layer networks of FitzHugh–Nagumo oscillators

with inhomogeneous topologies constructed by a small-world algorithm. In a triplex network with identical homogeneous layers, varying the interlayer coupling strength allows for regimes of relay synchronization, desynchronization, and complete synchronization. To check the robustness of these regimes, we have introduced topological inhomogeneities in the remote layers or the relay layer by randomly rewiring existing regular links and replacing them with random shortcuts with a probability p.

Complementary to the known scenarios for a regular nonlocally coupled ring network, we find a novel scenario with a direct transition from the regime of relay synchronization to the regime of complete synchronization without a desynchronized regime in between. This observation suggests that the introduction of inhomogeneities generally supports synchronization. Moreover, these findings are in agreement with results for one-layer networks[58] showing that regular ring networks exhibit poor synchronizability, which is significantly improved when random connections are added[59] or links are rewired within the network.[60] Our results further support previous observations that heterogeneous networks give rise to different transition scenarios between relay and full synchronizations.[61] Thus, we have extended those results from one layer toward multilayer systems and even generalized them for partial synchronization patterns such as chimera states.

Our findings demonstrate that random inhomogeneities in the network topology have a positive effect on the relay synchronization by increasing the parameter range where it is observed. This effect increases strongly with increasing link rewiring probability p. Comparing two cases of topological inhomogeneities, i.e., modification of the remote layers or the relay layer, respectively, we conclude that inhomogeneity in the remote layers is more advantageous for relay synchronization. In this case, relay synchronization can be observed for a wider range of the interlayer coupling strength.

Keeping the coupling range R in the initial network fixed and relatively large within the layers allows for the observation of chimera states with one incoherent domain in each layer. The case of more diluted topologies, i.e., a nonlocally coupled ring with a smaller coupling range, would result in chimera-like patterns with a larger number of alternating coherent and incoherent domains. But even for the large R we have used, an inhomogeneous relay layer can induce chimeras with two incoherent domains in all three layers.

ACKNOWLEDGMENTS

This work was supported by the Deutsche Forschungsgemeinschaft (DFG, German Research Foundation)—Project Nos. 163436311-SFB 910, 411803875, and 308748074.

DATA AVAILABILITY

The data that support the findings of this study are available within the article.

REFERENCES

[1] A. Pikovsky, M. Rosenblum, and J. Kurths, *Synchronization: A Universal Concept in Nonlinear Sciences* (Cambridge University Press, 2001).
[2] S. Boccaletti, G. Bianconi, R. Criado, C. I. del Genio, J. Gómez-Gardeñes, M. Romance, I. Sendiña Nadal, Z. Wang, and M. Zanin, Phys. Rep. **544**, 1 (2014).
[3] L. L. Gollo, C. R. Mirasso, M. Atienza, M. Crespo-Garcia, and J. L. Cantero, PLoS One **6**, e17756 (2011).
[4] I. Fischer, R. Vicente, J. M. Buldú, M. Peil, C. R. Mirasso, M. C. Torrent, and J. García-Ojalvo, Phys. Rev. Lett. **97**, 123902 (2006).
[5] A. Bergner, M. Frasca, G. Sciuto, A. Buscarino, E. J. Ngamga, L. Fortuna, and J. Kurths, Phys. Rev. E **85**, 026208 (2012).
[6] I. Leyva, I. Sendiña-Nadal, R. Sevilla-Escoboza, V. P. Vera-Avila, P. Chholak, and S. Boccaletti, Sci. Rep. **8**, 8629 (2018).
[7] J. Sawicki, I. Omelchenko, A. Zakharova, and E. Schöll, Phys. Rev. E **98**, 062224 (2018).
[8] M. Girvan and M. E. J. Newman, Proc. Natl. Acad. Sci. U.S.A. **99**, 7821 (2002).
[9] M. Moslonka-Lefebvre, C. A. Gilligan, H. Monod, C. Belloc, P. Ezanno, J. A. N. Filipe, and E. Vergu, J. R. Soc. Interface **13**, 20151099 (2016).
[10] V. Grimm, E. Revilla, U. Berger *et al.*, Science **310**, 987 (2005).
[11] J. C. Sprott, Phys. Lett. A **325**, 329 (2004).
[12] O. Woolley-Meza, C. Thiemann, D. Grady, J. J. Lee, H. Seebens, B. Blasius, and D. Brockmann, Eur. Phys. J. B **84**, 589 (2011).
[13] A. Cardillo, M. Zanin, J. Gòmez Gardeñes, M. Romance, A. Garcia del Amo, and S. Boccaletti, Eur. Phys. J. Spec. Top. **215**, 23 (2013).
[14] B. Bentley, R. Branicky, C. L. Barnes, Y. L. Chew, E. Yemini, E. T. Bullmore, P. E. Vétes, and W. R. Schafer, PLOS Comput. Biol. **12**, e1005283 (2016).
[15] F. Battiston, V. Nicosia, M. Chavez, and V. Latora, Chaos **27**, 047404 (2017).
[16] T. Chouzouris, I. Omelchenko, A. Zakharova, J. Hlinka, P. Jiruska, and E. Schöll, Chaos **28**, 045112 (2018).
[17] L. Ramlow, J. Sawicki, A. Zakharova, J. Hlinka, J. C. Claussen, and E. Schöll, Europhys. Lett. **126**, 50007 (2019).
[18] M. Kivelä, A. Arenas, M. Barthélemy, J. P. Gleeson, Y. Moreno, and M. A. Porter, J. Complex Netw. **2**, 203 (2014).
[19] M. De Domenico, C. Granell, M. A. Porter, and A. Arenas, Nat. Phys. **12**, 901 (2016).
[20] S. Boccaletti, A. N. Pisarchik, C. I. del Genio, and A. Amann, *Synchronization: From Coupled Systems to Complex Networks* (Cambridge University Press, 2018).
[21] P. J. Mucha, T. Richardson, K. Macon, M. A. Porter, and J. P. Onnela, Science **328**, 876 (2010).
[22] L. Tang, X. Wu, J. Lü, J. Lu, and R. M. D'Souza, Phys. Rev. E **99**, 012304 (2019).
[23] R. Berner, J. Sawicki, and E. Schöll, Phys. Rev. Lett. **124**, 088301 (2020).
[24] X. Zhang, S. Boccaletti, S. Guan, and Z. Liu, Phys. Rev. Lett. **114**, 038701 (2015).
[25] V. Nicosia, M. Valencia, M. Chavez, A. Díaz-Guilera, and V. Latora, Phys. Rev. Lett. **110**, 174102 (2013).
[26] L. V. Gambuzza, A. Cardillo, A. Fiasconaro, L. Fortuna, J. Gómez-Gardeñes, and M. Frasca, Chaos **23**, 043103 (2013).
[27] L. V. Gambuzza, M. Frasca, L. Fortuna, and S. Boccaletti, Phys. Rev. E **93**, 042203 (2016).
[28] L. Zhang, A. E. Motter, and T. Nishikawa, Phys. Rev. Lett. **118**, 174102 (2017).
[29] J. Sawicki, S. Ghosh, S. Jalan, and A. Zakharova, Front. Appl. Math. Stat. **5**, 19 (2019).
[30] M. Winkler, J. Sawicki, I. Omelchenko, A. Zakharova, V. Anishchenko, and E. Schöll, Europhys. Lett. **126**, 50004 (2019).
[31] R. W. Guillery and S. M. Sherman, Neuron **33**, 163 (2002).
[32] D. S. Bassett, A. Meyer-Lindenberg, S. Achard, T. Duke, and E. T. Bullmore, Proc. Natl. Acad. Sci. U.S.A. **103**, 19518 (2006).
[33] D. S. Bassett and E. T. Bullmore, Neuroscientist **12**, 512 (2006).
[34] L. M. Pecora, F. Sorrentino, A. M. Hagerstrom, T. E. Murphy, and R. Roy, Nat. Commun. **5**, 4079 (2014).
[35] Y. Kuramoto and D. Battogtokh, Nonlinear Phenom. Complex Syst. **5**, 380 (2002).
[36] D. M. Abrams and S. H. Strogatz, Phys. Rev. Lett. **93**, 174102 (2004).
[37] M. J. Panaggio and D. M. Abrams, Nonlinearity **28**, R67 (2015).
[38] E. Schöll, Eur. Phys. J. Spec. Top. **225**, 891 (2016).
[39] O. E. Omel'chenko, Nonlinearity **31**, R121 (2018).
[40] O. E. Omel'chenko and E. Knobloch, New J. Phys. **21**, 093034 (2019).
[41] E. Schöll, A. Zakharova, and R. G. Andrzejak, *Chimera States in Complex Networks*, Research Topics, Frontiers in Applied Mathematics and Statistics (Frontiers Media SA, Lausanne, 2020).

[42]N. C. Rattenborg, C. J. Amlaner, and S. L. Lima, Neurosci. Biobehav. Rev. **24**, 817 (2000).
[43]N. C. Rattenborg, B. Voirin, S. M. Cruz, R. Tisdale, G. Dell'Omo, H. P. Lipp, M. Wikelski, and A. L. Vyssotski, Nat. Commun. **7**, 12468 (2016).
[44]G. G. Mascetti, Nat. Sci. Sleep **8**, 221 (2016).
[45]A. R. Nikolaev, S. Gepshtein, P. Gong, and C. van Leeuwen, Cerebral Cortex **20**, 365 (2010).
[46]S. Ahn and L. L. Rubchinsky, Chaos **23**, 013138 (2013).
[47]S. Ahn, L. L. Rubchinsky, and C. C. Lapish, Cerebral Cortex **24**, 2553 (2014).
[48]P. Jiruska, M. de Curtis, J. G. R. Jefferys, C. A. Schevon, S. J. Schiff, and K. Schindler, J. Physiol. **591**(4), 7872013).
[49]V. K. Jirsa, W. C. Stacey, P. P. Quilichini, A. I. Ivanov, and C. Bernard, Brain **137**, 2210 (2014).
[50]H. Sakaguchi, Phys. Rev. E **73**, 031907 (2006).
[51]I. Omelchenko, O. E. Omel'chenko, P. Hövel, and E. Schöll, Phys. Rev. Lett. **110**, 224101 (2013).
[52]J. Hizanidis, V. Kanas, A. Bezerianos, and T. Bountis, Int. J. Bifurcation Chaos **24**, 1450030 (2014).
[53]I. Omelchenko, A. Provata, J. Hizanidis, E. Schöll, and P. Hövel, Phys. Rev. E **91**, 022917 (2015).
[54]J. Hizanidis, N. E. Kouvaris, G. Zamora-López, A. Díaz-Guilera, and C. Antonopoulos, Sci. Rep. **6**, 19845 (2016).
[55]R. FitzHugh, Biophys. J. **1**, 445 (1961).
[56]Note that the horizontal axis starts with $\sigma_i j > 0$, since we are not interested in the decoupled dynamics of the triplex network at very small $\sigma_i j$.
[57]D. J. Watts and S. H. Strogatz, Nature **393**, 440 (1998).
[58]A. Arenas, A. Díaz-Guilera, J. Kurths, Y. Moreno, and C. Zhou, Phys. Rep. **469**, 93 (2008).
[59]M. Barahona and L. M. Pecora, Phys. Rev. Lett. **89**, 054101 (2002).
[60]H. Hong, B. Jun Kim, M. Y. Choi, and H. Park, Phys. Rev. E **69**, 067105 (2004).
[61]B. Karakaya, L. Minati, L. V. Gambuzza, and M. Frasca, Phys. Rev. E **99**, 052301 (2019).